Integrative Biology

Accepted Manuscript

ROYAL SOCIETY OF CHEMISTRY

www.rsc.org/ibiology

Insight Statement for *Sonic hedgehog and neurotrophin-3 increase oligodendrocyte numbers and myelination after spinal cord injury*

We investigated gene delivery from biomaterial bridges, a platform technology to promote regeneration after SCI, as a tool to over-express trophic factors that activate endogenous oligodendrocyte progenitors to mediate myelination of regenerating axons. Localized, sustained expression of NT3 and SHH significantly increased the density of neuronal processes extending into bridges and myelination of these processes eight weeks after injury. Alone or in combination, NT3 and SHH increased the density of oligodendrocyte progenitors within bridges. Expression of NT3 enhanced myelination primarily by infiltrating Schwann cells, whereas SHH over-expression significantly increased myelination by oligodendrocytes. These results demonstrate that the combination of biomaterials and gene delivery provides sufficient physical and chemical cues to increase the density of regenerating axons and their subsequent myelination.

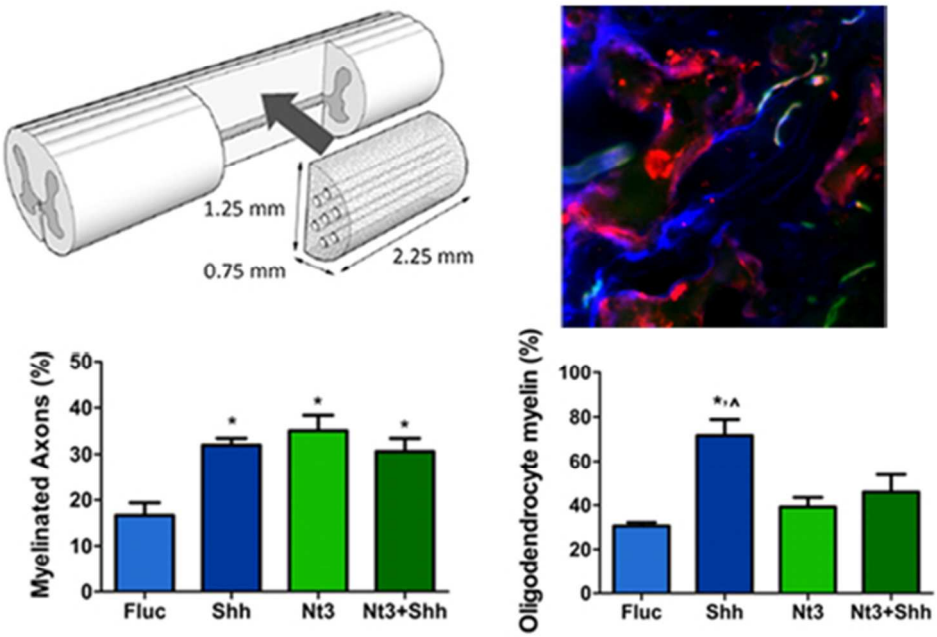

50x35mm (300 x 300 DPI)

Integrative Biology

RSCPublishing

ARTICLE

Sonic hedgehog and neurotrophin-3 increase oligodendrocyte numbers and myelination after spinal cord injury

Aline M. Thomas[a,‡], Stephanie K. Seidlits[b,c,‡], Ashley G. Goodman[b], Todor V. Kukushliev[b], Donna M. Hassani[d], Brian J. Cummings[e,f,g,h], Aileen J. Anderson[e,f,g,h], Lonnie D. Shea[*b,c,i,j,k]

Cite this: DOI: 10.1039/x0xx00000x

Received ooth January 2012,
Accepted ooth January 2012

DOI: 10.1039/x0xx00000x

www.rsc.org/

[‡]Denotes equal contribution.
*Correspondence should be addressed to L.D.S. (l-shea@northwestern.edu).

a Department of Biomedical Engineering, McCormick School of Engineering, Northwestern University, Evanston, IL, USA.
b Department of Chemical and Biological Engineering, McCormick School of Engineering, Northwestern University, Evanston, IL, USA
c Institute for BioNanotechnology in Medicine (IBNAM), Northwestern University, Chicago, IL, USA
d Department of Psychology, Weinberg College of Arts and Sciences, Northwestern University, Evanston, IL, USA
e Department of Physical Medicine and Rehabilitation, University of California, Irvine, CA, USA
f Department of Anatomy and Neurobiology, University of California, Irvine, CA, USA
g Sue and Bill Gross Stem Cell Center, Irvine, CA, USA
h Institute for Memory Impairments and Neurological Disorders (MIND), Irvine, CA, USA
i Center for Reproductive Science (CRS), Northwestern University, Evanston, IL, USA
j Robert H. Lurie Comprehensive Cancer Center, Northwestern University, Chicago, IL, USA
k Chemistry of Life Processes Institute (CLP), Northwestern University, Evanston, IL, USA

Spinal cord injury (SCI) results in loss of sensory and motor function below the level of injury and has limited available therapies. Multiple channel bridges have been investigated as a means to create a permissive environment for regeneration, with channels supporting axonal growth through the injury. Bridges support robust axon growth with myelination of the axons, and herein we investigated the cell types that are myelinating the axons and whether trophic factors can enhance myelination. Lentivirus encoding for neurotrophin-3 (NT3), sonic hedgehog (SHH) and the combination of these factors was delivered from bridges implanted into a lateral hemisection defect at T9/T10 in mice, and the response of endogenous progenitor cells within the spinal cord was investigated. Relative to control, the localized sustained expression of these factors significantly increased growth of regenerating axons into the bridge and enhanced axon myelination 8 weeks after injury. SHH decreased $Sox2^+$ cells and increased $Olig2^+$ cells, whereas NT3 alone or in combination with SHH enhanced $GFAP^+$ and $Olig2^+$ cells relative to control. For delivery of lentivirus encoding for either factor, we identified cells at various stages of differentiation along the oligodendrocyte lineage (e.g., $O4^+$, $GalC^+$). Expression of NT3 enhanced myelination primarily by infiltrating Schwann cells, whereas SHH over-expression substantially increased myelination by oligodendrocytes. Gene delivery represents a promising tool to direct activation and differentiation of endogenous progenitor cells for applications in regenerative medicine.

Introduction

Regeneration of spinal cord tissue can occur after injury when presented with inductive cues. Towards this goal, we have developed implantable bridges to support the long-distance growth of spared axons, defined as axons near the injury that did not undergo Wallerian-type degeneration, through the injury[1–4], and the delivery of neurotrophic factors promotes the additional extension of axons into the injury[5]; yet, these regenerating axons must be myelinated in order to appropriately relay the electrical signals needed to restore motor and sensory function. Following injury, myelinating cells in the spinal cord consist of Schwann cells and oligodendrocytes. Schwann cells from the peripheral nervous system (PNS) rapidly invade the spinal cord after injury and can spontaneously remyelinate spared axons in the central nervous system (CNS); however, Schwann cells generally do not form myelin sheaths thick enough to restore axonal conductance[6,7]. In contrast, oligodendrocytes, which normally produce myelin in the CNS, can myelinate multiple spared axons to enhance and integrate their conductance[8]. However, remyelination by mature oligodendrocytes rarely occurs, as few mature, pre-existing oligodendrocytes survive after spinal cord injury (SCI)[9–11] and are not capable of proliferation or extensive migration[11]. Instead, remyelination by CNS-derived cells is typically mediated by oligodendrocyte progenitors ($Olig2^+$, $NG2^+$), which reside in the adult spinal cord and are activated in response to injury[12–17]. However, myelination by oligodendrocyte progenitors is significantly hindered by the lack of pro-oligodendrogenic factors[18] and the abundance of factors that inhibit differentiation[18,19] in the tissue microenvironment following SCI.

Recent strategies to enhance the myelination of axons after SCI have targeted endogenous oligodendrocyte progenitors[18–23]. Oligodendrocyte myelination requires the migration, proliferation and differentiation of progenitors near to the injury[12,13,16,17]. Sonic hedgehog (SHH)[22–26] and neurotrophin-3 (NT3)[27–31] have been identified as factors that enhance the proliferation and differentiation of oligodendrocyte progenitors *in vitro* and *in vivo*. In addition, SHH promotes sparing of both neurons[32,33] and white matter[20] after CNS injury. SHH is also chemoattractant for neural-lineage progenitors during CNS development[34] and after injury[35]. NT3 is known to promote neuronal survival, sprouting of spared axons and regeneration of injured axons after injury[5,27,31]. Furthermore, NT3 amplifies the proliferation of oligodendrocyte progenitors *in vivo*[30,31]. These reports reveal inductive factors can increase progenitor presence after SCI; however, the ability of these endogenous progenitors to differentiate into mature oligodendrocytes and subsequently myelinate large numbers of regenerating axons remains unknown.

In this report, we investigated NT3 and SHH individually and in combination for their ability to enhance the recruitment, proliferation and differentiation of oligodendrocyte progenitors and their ability to myelinate large numbers of regenerating axons that are growing through a biomaterial bridge implanted into the injury. Previously, we fabricated multiple channel bridges from biodegradable poly(lactide-co-glycolide) (PLG) containing a high density of linear channels that enabled the guidance of regenerating axons across the injury site when implanted into a lateral hemisection lesion in the mouse spinal cord[2,36]. In addition, the bridge contains a network of interconnected pores that permitted the rapid infiltration of multiple cell types from the adjacent tissue[1–4]. Functionalization of these bridges with lentivirus provided robust, sustained transgene expression after SCI[5,36,37]. Axons are completely severed in the lesion before bridge implantation; thus axons extending through the bridge can be attributed to regeneration of injured axons or sprouting of contralateral axons and are not spared axons originating from the injury site. The capacity of these axons regenerating through the injury to contribute to restoration of circuitry within the spinal cord will require re-myelination to establish conduction; therefore, our analysis focused on the recruitment and differentiation of endogenous glial progenitor cells within the bridge implants, and on the extent and source of myelination within the bridge. Using a mouse model, lentiviral delivery was employed to obtain localized and persistent expression of SHH and/or NT3, and histology was employed to determine the characteristics of the regenerating tissue. Lentiviral delivery allowed for sustained expression of one or more factors for the duration of the study. Furthermore, expression is greatest within the implant, with decreasing concentrations in adjacent spinal cord segments that creates a concentration gradient that may direct cell migration towards the implant. The ability for the biomaterial and localized gene delivery to modulate the local environment represents a significant advance towards regenerating spinal circuitry through the injured spinal cord.

Results

Transgene expression in the spinal cord

Initial studies characterized the location of transgene expression following bridge-mediated lentivirus delivery. Bridges were implanted into a lateral hemisection model at T9-T10 (**Fig. 1a, b**), with extensive cell infiltration and integration with the host tissue[1–4]. Additionally, delivery of lentivirus from these bridges has promoted transgene expression that exceeded 60 days[36]. Lentiviral particles (~5 x 10^7 LP) encoding Firefly luciferase (FLuc) were delivered from PLG bridges and localization of transgene expression was assessed 4 weeks after injury. Upon extraction of the spinal cord, more than half of the transgene expression resided within the implantation site (**Fig. 1c**). Additionally, over 80% of transgene expression was within two vertebrae adjacent to the implantation site. This distribution of transgene expression demonstrates the ability to locally deliver gene therapy vectors. We confirmed that expression is sustained over at least 60 days (8 weeks) when two lentiviral vector encoding for different transgenes (FLuc and green fluorescent protein, GFP) were simultaneously delivered from a single bridge platform (**Fig. 1d**). Co-expression of both transgenes was confirmed by immunohistochemistry in spinal cords extracted 8 weeks after injury (**Fig. 1e, f**). Most cells expressing either GFP or FLuc expressed both transgenes.

Recruitment and differentiation of endogenous progenitors

Lentivirus from the bridge was subsequently employed to express NT3, SHH or a combination of these factors in order to modulate the tissue microenvironment within and adjacent to the implantation site. An analysis of sparing of grey and white matter contra-lateral to the injury was performed. The contralateral tissue had damage to both the grey and white matter in all conditions, and expression of NT3, SHH, or their combination did not significantly impact the extent of damage to the grey and white matter in the contralateral tissue. Here, we define "damaged" tissue as tissue that no longer presents the normal morphology of healthy spinal cord tissue. In healthy spinal cord, the "butterfly" shape of the grey matter is visible and myelinated axon bundles are distributed throughout the white matter. In addition, the total cell number in the bridges was similar for all conditions (**Supp. Fig. 1**).

Staining of tissue sections for adult spinal cord, neural lineage-progenitors ($Sox2^+$) were present throughout the bridge implants (**Fig. 2a-e**). In the case of SHH over-expression, a significantly decreased number of $Sox2^+$ cells was observed relative to delivery of the control vector (FLuc) (**Fig. 2f**). NT3 over-expression exhibited a trend toward reducing the number of $Sox2^+$ cells relative to control, though the decrease was not significant. The combination of SHH and NT3 over-expression produced levels of $Sox2^+$ cells that were approximately similar to controls. $Sox2^+$ progenitor cells in the process of differentiating along astrocyte or oligodendrocyte lineages may co-express glial fibrillary acidic protein (GFAP) and cytoplasmic $Olig2$[38–41] or nuclear $Olig2$[16,42], respectively. Thus, we assessed co-localization of Sox2 and these markers. Overlap of these markers within single cells, as visualized from widefield fluorescence imaging, was confirmed using confocal microscopy (**Supp. Fig. 2**). The percentage of $Sox2^+$ cells that were also $GFAP^+$ and/or $Olig2^+$ was similar across experimental conditions (**Fig. 2g**), with uncommitted neural progenitor cells ($Sox2^+/GFAP^-/Olig2^-$) trending toward the greatest percentage of $Sox2^+$ cells with SHH or NT3/SHH expression. Likewise, there were no significant differences in the density of $Sox2^+$ cells that were also $GFAP^+$ and/or $Olig2^+$ across experimental conditions (**Fig. 2h**). However, the data again indicate a trend towards increased presence of uncommitted neural progenitors. Finally, we note that a trend towards increased proliferation of $Sox2^+$ cells with expression of NT3 or NT3/SHH in combination, though the levels were not significant (**Supp. Fig. 3a**).

Presence of glial-restricted precursors was investigated within the bridge area by immunostaining for Olig2 (**Fig. 3a-e**). Over-expression of SHH, NT3, or their combination increased the number of cells expressing nuclear Olig2 by 5 to 9-fold relative to control (**Fig. 3f**). As Olig2 expression was confined to the nucleus in the majority of $Olig2^+$ cells, the percentage of both $GFAP^+/Olig2^+$ and $Sox2^+/Olig2^+$ cells was relatively unaffected by expression of any factor. However, a trend was observed for increased percentage of $GFAP^-/Sox2^-/Olig2^+$ cells with expression of SHH, NT3, or their combination (**Fig. 3g**). Similarly, no significant differences were observed in the densities of $GFAP^+/Olig2^+$, $Sox2^+/Olig2^+$ or $GFAP^-/Sox2^-/Olig2^+$ cells across conditions (**Fig. 3h**). However, there were trends indicating the presence of fewer $Sox2^+/Olig2^+$ cells in NT3 only case and more $GFAP^-/Sox2^-/Olig2^+$ cells in the SHH only case. $GFAP^-/Sox2^-/Olig2^+$ likely represent oligodendroctye precursor cells or immature oligodendrocytes[43]. The number of $Olig2^+/Ki67^+$ cells (proliferative oligodendrocyte precursors) demonstrated a trend toward increased proliferation in the presence of SHH, NT3, or the combination (≈3 to 5 fold increase relative to FLuc) (**Supp. Fig. 3b**). Consistent with Olig2 staining, staining for NG2 was also observed within the bridges, which stains glia-restricted progenitors, yet may also stain other infiltrating cell types, such as meningeal fibroblasts, non-myelinating Schwann cells, and macrophages (**Supp. Fig. 4a-d**)[44,45]. In addition, markers for oligodendrocyte progenitors at later stages of maturation were also observed, such as O4 (**Supp. Fig. 4e-h**) and galactosylceramidase (GalC) (**Supp. Fig. 4i-l**), which stain immature oligodendrocytes and immature and mature oligodendrocytes respectively.

Astrocytes were identified by staining for GFAP, which indicated these cells were present at the injury (**Fig. 4a-e**), primarily at the interface of the bridge and host tissue. The density of GFAP+ cells in the bridge significantly increased when NT3 was over-expressed, regardless of whether SHH was also over-expressed (Fig. 4f). The number of $Ki67^+/GFAP^+$ cells (proliferative astrocytes, astrocyte precursors or proliferative neural progenitors) also significantly increased when NT3 was overexpressed (**Supp. Fig. 3c**), again independent of SHH delivery. In the scar adjacent to the bridge, the presence of GFAP was unaffected by factor delivery. As numbers of $GFAP^+/Sox2^+/Olig2^-$ cells (astrocyte precursors) remained low and unvarying across conditions (**Fig. 2g, 2h**), the additional $GFAP^+$ cells with NT3 expression were most likely mature, reactive astrocytes.

Axon regeneration, myelination, and sparing

Both unmyelinated (neurofilament-160, NFM+) and myelinated (NFM^+/myelin basic protein, MBP^+) nerve fibers were present throughout the bridge in control animals that over-expressed Fluc (**Fig. 5a-e**). NFM^+ staining was typically confined to individual, unbundled nerve fibers. Control animals had approximately 1500 neurites/mm^2 (**Fig. 5f**), 17% of which were myelinated (**Fig. 5g**). This observation has previously been attributed to the bridge architecture, consisting of linear channels and interconnected pores[2], which allows for the infiltration of host cells that create a growth inductive environment. Regenerating axons typically appeared bundled as pairs, triplicates or more, consistent with previous reports[2,3,5] (**Fig. 5b-e**). Upon expression of SHH or NT3 alone, the total number of axons that extended into the middle of the bridge significantly increased by approximately 2-fold relative to control (**Fig. 5f**). Similar to axon number, the number of myelinated axons (NFM^+/MBP^+) also significantly increased in the presence of either SHH or NT3 by approximately 7-fold and 6-fold respectively, relative to controls. The tandem expression of SHH and NT3 did not further enhance the number of axons or myelinated axons in the bridges. The percentage of myelinated axons, which was determined from the ratio of the number of NFM+/MBP+ axons divided by the number of NFM+ axons, was similar for SHH, NT3, or the combination, and was significantly increased relative to control (**Fig. 5g**).

The source of myelination in the bridge was investigated by immunostaining to identify whether remyelinated fibers were ensheathed by Schwann cell ($NFM^+/MBP^+/P0^+$) (**Fig. 6a-e**) or oligodendrocyte-derived myelin ($NFM^+/MBP^+/P0^-$) (**Fig. 6f**). In control animals, significantly fewer numbers of myelinated axons were observed relative to delivery of NT3 or SHH alone or their combination (**Fig. 6f**). In the controls, the percentage of these myelinated fibers ensheathed by oligodendrocytes-derived myelin was 31% (**Fig. 6g**), with the percentage determined from the ratio of the number of MBP+/PO+ axons divided by the number of MBP+ axons,. Over-expression of SHH resulted in significantly greater percentage of oligodendrocyte-myelinated fibers (72%) compared to control (**Fig. 6g**). Over-expression of NT3 resulted in an increase of both oligodendrocyte and Schwann cell myelin relative to control

(**Fig. 6f,g**), with oligodendrocytes myelinating approximately 40% of myelinated fibers. Furthermore, NT3 expression significantly increased the percentage of Schwann cell-myelinated fibers compared to all other groups (**Fig. 6g**). NT3 has been shown *in vitro* to promote the migration of Schwann cells[46], which may influence myelination. Additionally, the combination of SHH and NT3 over-expression also increased both Schwann cell and oligodendrocyte-derived myelin relative to control, with 45% of axonal fibers within the bridge implant ensheathed by oligodendrocyte-derived myelin (**Fig. 6g**). However, the combination of NT3 and SHH delivery resulted in a significantly lower percentage of oligodendrocyte-myelinated fibers when compared to SHH alone.

Discussion

We investigated myelination of regenerating axons by host cells recruited into multiple channel PLG bridges implanted into a mouse lateral hemisection spinal cord lesion. We have previously reported the ability of the bridge architecture to encourage axon regeneration after SCI due to the enhanced infiltration of multiple cell types and guidance of severed axons through linear channels[1–4]. Moreover, lentiviral delivery from the bridges resulted in sustained, localized transgene expression capable of altering the injury microenvironment[2,5,36]. In particular, delivery of lentivirus encoding for NT3 further increased the number of axons extending through the bridge implant[5]. Notably, lentiviral delivery from PLG bridges provides a platform for long-term, localized production of therapeutic proteins, which is difficult to achieve and often requires the use of osmotic pumps. Unlike other viral vectors, lentivirus does not influence the cellular behavior of progenitors[47] nor invoke a significant inflammatory response[48]. Lentiviral vectors exhibit the same physical properties, independent of the encoding gene. Therefore, in contrast to protein delivery, the same delivery system can be applied to deliver multiple vectors encoding various regenerative factors without modification to the biomaterial platform. In these studies, lentiviral vectors encoding two distinct transgenes were delivered from PLG bridges and transgene expression altered the local environment for at least 8 wks after injury to promote axonal regeneration and remyelination. This combination of biomaterials and gene delivery technology have provided a means for local delivery of multiple regenerative factors. Furthermore, expression of these factors resulted in a gradient along the spinal cord, with the greatest concentration at the implantation site, which was sustained for at least 60 days. Approximately 50% of transgene expression was localized at the level of the implant (T9/10), with an additional 30% in adjacent segments (T7/8 and T11/12). This steep decrease in expression in either direction along the spinal cord resulted in a gradient of the expressed regenerative factors. Gradients of inductive factors, and specifically of NT-3 and SHH, are well-established for their role in directing cell movement during development[34,35,49-52] and maintenance of this gradient may contribute to the recruitment and differentiation of progenitor cells within the spinal cord.

The bridge implants provide a defined space for analysis of progenitor cell recruitment to the injury site. The contribution of endogenous progenitor cells to repair after SCI has been challenging to characterize in many common injury models. However, in these studies the bridges are acellular at the time of implantation so that any cells present in the bridge at the time of extraction must have migrated from the host tissue. Likewise, as axons in the hemisection injury model are completely severed prior to bridge implantation, any axons observed entering the implant space can be attributed to either regeneration of injured axons or novel sprouting of axons from the contralateral tissue. The contribution of these axons to restoring circuitry within the spinal cord requires remyelination of the axons. These studies focused on histological investigation of endogenous progenitor cells and axonal processes that migrate or extend into the bridge from the adjacent spinal cord tissue. Spontaneous rewiring of corticospinal circuits is observed that results from sprouting of spared axons[53-57]. In contrast, the long-distance regeneration of axons through an injury and subsequent myelination remains a substantial challenge, yet promises to enhance recovery. The analysis of regeneration herein demonstrated the potential of axons to extend through a spinal cord lesion and the potential for influencing the differentiation of endogenous progenitor cells to facilitate tissue repair and restoration of function.

In bridges lacking lentivirus encoding for inductive factors, the abundance of progenitor cells (identified as $Sox2^+$ and/or $Olig2^+$) and proliferating progenitors (co-labeled as $Ki67^+$) within the bridges was relatively low in the absence of inductive factors. Furthermore, the paucity of immature ($O4^+$) and mature ($GalC^+$) oligodendrocytes along with the lack of axonal myelination within the bridges indicates that $Sox2^+$ and $Olig2^+$ progenitor cells did not effectively undergo differentiation into functional, myelinating oligodendrocytes. Results reported herein with the bridge alone are consistent with previous reports that few oligodendrocyte precursors, which are required for remyelination of axons[17], are present[12–16]. This lack of immature oligodendrocytes near the injury may have limited remyelination by glia of CNS origin. Thus, in our control bridges (no lentivirus), comparable levels of myelination by oligodendrocytes and infiltrating Schwann cells were observed.

Addition of lentivirus encoding for NT3 to the bridge sufficiently altered the injury environment to enhance recruitment and differentiation of oligodendrocyte precursors and enhanced myelination of regenerating nerve fibers, consistent with previous report in rat models[5,58]. NT3 over-expression has promoted robust regeneration of axons across the injury site and increased axonal myelination; however, the majority of these axons remain unmyelinated[5,58]. After injury, remyelination occurs when endogenous progenitor cells migrate towards the injury, proliferate and differentiate into mature oligodendrocytes[12–17]. The improved myelination with NT3 expression can be attributed to increases in both Schwann cell- and oligodendrocyte-derived myelin at the injury, with increases in Schwann cell-derived myelin greater than that of oligodendrocyte-derived myelin. NT3 likely enhanced recruitment of Schwann cells into the bridge[46]. An increase in $Olig2^+$ staining was observed within the bridge for NT3 over-expression (**Supp. Fig. 4**), suggesting recruitment of oligodendrocyte progenitors; however, NT3 was apparently insufficient to promote their differentiation into mature, myelinating oligodendrocytes.

Delivery of SHH-encoding lentiviral vectors from the bridge significantly increased numbers of myelinated axons at the injury relative to NT3 over-expression and negative controls, and significantly amplified the percentage of axons myelinated by CNS-derived oligodendrocytes rather than PNS-derived Schwann cells. We hypothesized that SHH would enhance

myelination after injury by improving recruitment of oligodendrocyte progenitors to the lesion and subsequently promoting their maturation into functional, myelinating oligodendrocytes. This hypothesis was supported by the results that over-expression of SHH increased the numbers of oligodendrocyte progenitors ($Olig2^+$) recruited to the injury while simultaneously maintaining low numbers of astrocytic cells ($GFAP^+$) at levels similar to controls and significantly reduced relative to NT3 over-expression. Expression of SHH- or NT3-encoding lentivirus alone resulted in a decreased presence of $Sox2^+$ progenitor cells, while simultaneous delivery of both SHH- and NT3-encoding lentivirus increased the presence of these neural-lineage progenitors relative to either factor alone. These findings suggest that combinatorial delivery of multiple inductive factors can substantially perturb the recruitment of endogenous progenitor cells at various stages of differentiation.

Previous studies have reported that SHH delivery increases both the presence and proliferation of endogenous progenitors after SCI ($NG2^+$ [23] and $nestin^+$ [21] cells) or traumatic brain injury ($Olig2^+$ cells)[26]. Although we observed a significant increase in the numbers of progenitor cells with SHH over-expression, we did not observe an effect of SHH on proliferation. However, these previous studies measured proliferation within 3 wks of injury[20,21,23], while the data presented in this manuscript were acquired 8 wks after injury. Thus, it is possible that NT3 or SHH over-expression promoted progenitor proliferation at relatively soon after SCI, while by 8 wks progenitors may have exited the cell cycle and proceeded toward differentiation.

The combined delivery of NT3 and SHH resulted in axon extension and myelination similar to NT3 alone, despite the presence of SHH. This result suggests that NT3 expression may inhibit oligodendrocyte maturation, which is supported by reports that NT3 acts to maintain oligodendrocyte progenitors in a proliferative state[30,59]. Alternatively, NT3 may be more effective at promoting myelination by Schwann cells than by oligodendrocytes. It is also possible that over-expression of inductive factors may have influenced glial progenitors from the PNS to differentiate into CNS-like glia. PNS-derived glial progenitors can differentiate to myelinate CNS axons and express markers typically associated with myelinating oligodendrocytes (e.g., GalC)[60]. Likewise, these trans-diffentiated cells do not express P0, a common marker for Schwann cell-derived myelin. Thus, SHH over-expression may promote myelination from CNS progenitors or trans-differentiation of PNS progenitors. In all experimental conditions, the majority of myelinated axons in the bridge appeared in the regions closest to the contralateral tissue (**Supp. Fig. 1a**), suggesting that oligodendrocyte progenitors and Schwann cells (or PNS progenitors) migrated into the injury from the adjacent host spinal cord and dorsal root ganglia, respectively. This pattern of myelination indicates that the ability of glial cells to migrate within close proximity of regenerating axons may have substantial effects on remyelination after injury and that additional recruitment of these cells may be beneficial.

Conclusions

We report the ability of two inductive factors (NT3 and SHH) to promote axon extension and remyelination by endogenous progenitor cells following SCI. In these studies both axon extension and myelination were increased to similar levels when NT3 and SHH were delivered alone or in combination, when compared to negative controls. However, SHH promoted greater myelination by oligodendrocytes, consistent with its ability to increase the presence of oligodendrocyte progenitor cells ($Olig2^+$). In contrast, NT3 promoted myelination by both CNS-derived oligodendrocytes and PNS-derived Schwann cells. Overall, we have demonstrated that lentivirus delivered from implanted bridges provides a viable strategy to provide long-term, combinatorial delivery of regenerative factors that target multiple barriers to regeneration.

Experimental

Heparin-modified PLG bridges

Porous bridges, with a porosity of 90%, sized for a mouse spinal cord hemisection lesion were formed based on a previously established technique[2]. In brief, a 1:1 mixture of PLG (75:25 ratio of D,L-lactide to L-glycolide, inherent viscosity: 0.76 dL/g; Lakeshore Biomaterials, Birmingham, AL, USA) and 63-106 μm salt coated cylindrical sugar fibers drawn from 220˚C caramelized sucrose, was packed into a mold, was equilibrated under 800 psi of carbon dioxide for 16 hours and was then released at 60 psi/min to foam into the final structure. The bridges were sectioned, leached 15 min in distilled water, dried and stored desiccated at room temperature until use.

Bridges were modified by first drying chitosan (8183 mol. wt., Sigma Aldrich, St. Louis, MO, USA) onto the surface and then immersing the bridge for 2 hours into 1 mL of 1 M 2-(N-morpholino)ethanesulfonic acid (MES, Sigma Aldrich) buffer in the presence of 9 mg 1-Ethyl-3-[3-dimethylaminopropyl] carbodiimide hydrochloride (EDC, CreoSalus Inc., Louisville, KY, USA) and 6 mg N-hydroxysulfosuccinimide (NHS, Research Organics, Cleveland, OH, USA). Heparin (180 USP/mg, Sigma Aldrich) was attached onto the chitosan-modified PLG by drying heparin onto the chitosan-modified bridge and then immersing the bridge into the above EDC/NHS in MES solution overnight[36]. The modified bridges were washed with distilled water, dried and stored desiccated at room temperature for up to one week before use.

Lentivirus production

Human embryonic kidney cells (HEK 293T, ATCC CRL-11268) cells were cultured in Dulbecco's modified eagle medium containing 10% fetal bovine serum and 1% penicillin-streptomycin. All cell culture materials were purchased from Life Technologies (Carlsbad, CA, USA). Lentivirus was prepared using a previously established technique[25,36,37]. Cells were co-transfected with vectors encoding plenti-CMV-Firefly luciferase, plenti-CMV-human SHH or plenti-CMV-human NT3 and the following packaging vectors: pMDL-GagPol, pRSV-Rev, pIVSVSV-G using Lipofectamine 2000 (Life Technologies). Supernatant was collected after 48 hours, concentrated in PEG-it (SystemBiosciences, Mountain View, CA) for 24 hours, precipitated using ultracentrifugation and resuspended in PBS. Titer was determined using a qPCR lentivirus titer kit (Applied Biological Materials, Inc., Richmond, BC, Canada).

Gene expression *in vivo*

For *in vivo* delivery, lentivirus (~1.5 x 10^7 particles total) was pipetted directly onto a porous, 7-channel PLG bridge, allowed to adsorb onto the bridge surface and stored at –80 ºC until use. Mice were treated according the Animal Care and use Committee guidelines at Northwestern University and all animal procedures were pre-approved by the Committee. SCI surgery and bridge implantation was performed as previously described (n = 4 per condition)[2]. C57Bl6 females (4-6 wks old, Charles River, Wilmington, MA, USA) were anesthetized using isoflurane (2%). A dorsal laminectomy was performed at T9-T10 for bridge implantation into a 2.25 mm long hemisection lesion. The injury site was covered by Gelfoam and stabilized by suturing the dorsal muscles and stapling the skin to close the wound. Baytril (enrofloxacin 2.5 mg/kg, once a day for 14 days), buprenorphine (0.01 mg/kg, twice a day for 3 days), and lactate ringer solution (5 mL/100 g, once a day for 5 days) were subcutaneously administered post-operatively. Bladders were expressed twice daily until urinary function recovered.

To quantify luciferase expression, spinal cords were extracted 4 weeks after implantation, sectioned every two vertebrae along the length of the spinal column, and frozen at -80 ˚C. Thawed sections were homogenized in 100 µL of 1x reporter lysis buffer (Promega, Madison, WI, USA), centrifuged at 14,000 rpm for 10 min at 4 ˚C, and supernatant collected. Luciferase activity in the supernatant was then assessed by measuring light production in the presence of the substrate D-luciferin (Promega) using a luminometer (10 s integration time).

Immunohistochemistry

Spinal cords containing bridge implants were extracted 8 weeks after SCI and flash frozen in isopentane. Spinal cords were then cyrosectioned transversally (18 µm sections). Sections in the middle of the bridge were used for all analyses. Immuno-stained tissue sections were imaged using both widefield (Leica DMRB, Wetzlar, Germany) and confocal (Leica SP5) fluorescence microscopes. Widefield images were acquired using standard fluorescence filter cube sets with a 16-bit, monochromatic CCD (CoolSNAP, Photometrics, Tuscon, AZ, USA). Hoescht$^+$ nuclei were quantified by selecting positive area using a color threshold and summing the number of particles after applying the watershed feature in FIJI/ImageJ (NIH, Bethesda, MD, USA).

The following antibodies were used for primary detection: anti-Ki67 (1:300, ab16667, AbCam, Cambridge, MA, USA), anti-Ki67 (1:100, sc-7846, Santa Cruz Biotechnology, Santa Cruz, CA, USA), anti-GFAP (1:1000, G3893, G4546, Sigma Aldrich), anti-GFAP (1:1000, ab53554, AbCam), anti-CS56 (1:200, C8035, Sigma Aldrich), anti-NG2 (1:200, ab5320, Millipore, Billerica, MA), anti-Sox2 (1:400, ab97959, AbCam), anti-Olig2 (1:200, MABN50, Millipore), anti-GalC (1:200, MAB342, Millipore), anti-O4 (1:200, MAB345, Millipore), anti-NFM (1:1000, MAB1621, Millipore), anti-MBP (1:1000, sc-13914, Santa Cruz Biotechnology), anti-P0 (1:500, MPZ, Aves Labs, Tigard, OR, USA). Species-specific antibodies were used for secondary detection (1:500-1:1000, Life Technologies, unless otherwise noted): AlexaFluor 488 goat anti-rabbit IgG (A-11034), AlexaFluor 555 goat anti-rabbit IgG (A-21429), AlexaFluor 488 goat anti-mouse IgG (A-11029), AlexaFluor 555 goat anti-mouse IgG (A-21424), AlexaFluor 488 goat anti-mouse IgM (A-21042), AlexaFluor 488 donkey anti-goat IgG (A-11055), AlexaFluor 555 donkey anti-goat IgG (A-21432), AlexaFluor 546 donkey anti-goat IgG (A-11056), AlexaFluor 633 donkey anti-goat IgG (A-21082), AlexaFluor 647 donkey anti-goat IgG (A-21447), AlexaFluor 555 donkey anti-mouse IgG (A-31570), AlexaFluor 647 donkey anti-mouse IgG (A-31571), fluorescein anti-chicken IgY (F-1005, Aves Labs).

Numbers of immuno-positive cells and axons were quantified manually by two researchers independently. Co-staining for multiple markers was always assessed by evaluating overlap of pixels above a set threshold in images acquired over identical sample areas. Co-localization of Sox2, GFAP and Olig2, was evaluated to determine the numbers of neural progenitors, astrocytes and oligodendrocyte progenitors, respectively. Overlap of markers within single cells was confirmed using confocal fluorescence imaging. Because the PLG material generally exhibits high background, cells were counted as Olig2, Sox2 or GFAP positive only when appearance of those markers spatially overlapped Hoescht$^+$ nuclei (**Supp. Fig. 5**).

To assess the numbers of regenerated and myelinated axons, a double stain for NFM and MBP was performed. Only axons within the bridge were included and axon counts were normalized to bridge area (**Supp. Fig. 6a-c**). The fraction of myelinated axons was calculated as the ratio of MBP^+/NFM^+ axons divided by the total number of axons (NFM+). To assess the source of the myelin, a triple stain of NFM, MBP and P0 was performed. $MBP^+/P0^-/NFM^+$ axons were considered to be myelinated by oligodendrocytes while $MBP^+/P0^+/NFM^+$ axons were considered to be myelinated by Schwann cells (**Supp. Fig. 6d-g**). The fraction of axons ensheathed with CNS-derived myelin was calculated as $MBP^+/P0^-/NFM^+$ axons divided by MBP^+/NFM^+ axons. Sparing of spinal cord tissue was quantified by measuring the area of abnormal or pathological tissue contralateral to the injury in transverse sections. Area was normalized to the length of the scar boundary dividing the lesion and the contralateral tissue.

Statistics

Multiple comparisons pairs were analyzed using a one-way or two-way ANOVA with a Bonferonni post-hoc test as appropriate. Significance was defined at a level of $p<0.05$ unless otherwise indicated.

Acknowledgements

This work was supported by the NIH (RO1 EB005678, R21 EB006520, RO1 EB003806, R01 CA173745, F32 NS081961 (SKS)). *In vivo* bioluminescence imaging work was performed at the Northwestern University Center for Advanced Molecular Imaging generously supported by NCI CCSG P30 CA060553 awarded to the Robert H Lurie Comprehensive Cancer Center. Confocal microscopy was performed at the Northwestern University Biological Imaging Facility. Technical support for animal studies from the Northwestern University Center for Comparative Medicine.

References

1 L. De Laporte, Y. Yang, M.L. Zelivyanskaya, et al. "Plasmid releasing multiple channel bridges for transgene expression after spinal cord injury," *Mol Ther*, 2009, **17**(2), 318-326.

2 A.M. Thomas, M.B. Kubilius, S.J. Holland, et al. "Channel density and porosity of degradable bridging scaffolds on axon growth after spinal injury," *Biomaterials*, 2013, **34**(9), 2213-2220.

3 H.M. Tuinstra, D.J. Margul, A.G. Goodman, et al. "Long-term characterization of axon regeneration and matrix changes using multiple channel bridges for spinal cord regeneration," *Tissue Eng A,* 2014, published online Dec. 11, 2013.

4 Y. Yang, L. De Laporte, M.L. Zelivyanskaya, et al. "Multiple channel bridges for spinal cord injury: cellular characterization of host response," *Tissue Eng Part A,* 2009, **15**(11), 3283-3295.

5 H.M. Tuinstra, M.O. Aviles, S. Shin, et al. "Multifunctional, multichannel bridges that deliver neurotrophin encoding lentivirus for regeneration following spinal cord injury," *Biomaterials*, 2012, **33**(5), 1618-1626.

6 J.D. Guest, E.D. Hiester and R.P. Bunge. "Demyelination and Schwann cell responses adjacent to injury epicenter cavities following chronic human spinal cord injury," *Exp Neurol,* 2005, **192**(2), 384-393.

7 B.E. Powers, J. Lasiene, J.R. Plemel, et al. "Axonal thinning and extensive remyelination without chronic demyelination in spinal injured rats," *J Neurosci*, 2012, **32**(15), 5120-5125.

8 Y. Yamazaki, Y. Hozumi, K. Kaneko, et al. "Oligodendrocytes: Facilitating axonal conduction by more than myelination," *Neuroscientist*, 2010, **16**(1), 11-18.

9 G.L. Li, M. Farooque, A. Holtz and Y. Olsson. "Apoptosis of oligodendrocytes occurs for long distances away from the primary injury after compression trauma to rat spinal cord," *Acta Neuropathol,* 1999, **98**(5), 473-480.

10 S. Casha, W.R. Yu and M.G. Fehlings. "Oligodendroglial apoptosis occurs along degenerating axons and is associated with FAS and p75 expression following spinal cord injury in the rat," *Neurosci,* 2001, **103**(1), 203-218.

11 S.D. Grossman, L.J. Rosenberg and J.R. Wrathall. "Temporal–spatial pattern of acute neuronal and glial loss after spinal cord contusion," *Exp Neurol,* 2001, **168**(2), 273-282.

12 J.M. Gensert and J.E. Goldman. "Endogenous progenitors remyelinate demyelinated axons in the adult CNS," *Neuron* ,1997, **19**(1), 197-203.

13 H. Yang, P. Lu, H.M. McKay, et al. "Endogenous neurogenesis replaces oligodendrocytes and astrocytes after primate spinal cord injury," *J Neurosci*, 2006, **26**(8), 2157-2166.

14 S. Mi, R.H. Miller, W. Tang, et al. "Promotion of central nervous system remyelination by induced differentiation of oligodendrocyte precursor cells," *Ann Neurol,* 2009, **65**(3), 304-315.

15 D.L. Sellers, D.O. Maris and P.J. Horner. "Postinjury niches induce temporal shifts in progenitor fates to direct lesion repair after spinal cord injury," *J Neurosci*, 2009, **29**(20), 6722-6733.

16 F. Barnabé-Heider, C. Goritz, H. Sabelström, et al. "Origin of new glial cells in intact and injured adult spinal cord," *Cell Stem Cell,* 2010, **7**(4), 470-482.

17 Y. Yang, R. Lewis and R.H. Miller. "Interactions between oligodendrocyte precursors control the onset of CNS myelination," *Develop Bio,* 2011, **350**(1), 127-138.

18 Y. Wang, X. Cheng, Q. He, et al. "Astrocytes from the contused spinal cord inhibit oligodendrocyte differentiation of adult oligodendrocyte precursor cells by increasing the expression of bone morphogenetic proteins," *J Neurosci,* 2011, **31**: (16), 6053-6058.

19 J. Chen, S.Y. Leong and M. Schachner. "Differential expression of cell fate determinants in neurons and glial cells of adult mouse spinal cord after compression injury," *Eur J Neurosci,* 2005, **22**: (8), 1895-1906.

20 N.C. Bambakidis and R.H. Miller. "Transplantation of oligodendrocyte precursors and sonic hedgehog results in improved function and white matter sparing in the spinal cords of adult rats after contusion," *Spine J,* 2004, **4**(1), 16-26.

21 N.C. Bambakidis, E.M. Horn, P. Nakaji, et al. "Endogenous stem cell proliferation induced by intravenous hedgehog agonist administration after contusion in the adult rat spinal cord," *J Neurosurg Spine,* 2009, **10**(2), 171-176.

22 N. Lowry, S.K. Goderie, M. Adamo, et al. "Multipotent embryonic spinal cord stem cells expanded by endothelial factors and Shh/RA promote functional recovery after spinal cord injury," *Exp Neurol,* 2008, **209**(2), 510-522.

23 N. Lowry, S.K. Goderie, P. Lederman, et al. "The effect of long-term release of Shh from implanted biodegradable microspheres on recovery from spinal cord injury in mice," *Biomaterials,* 2012, **33**(10), 2892-2901.

24 K. Lai, B.K. Kaspar, F.H. Gage and D.V. Schaffer. "Sonic hedgehog regulates adult neural progenitor proliferation in vitro and in vivo," *Nature Neurosci,* 2003, **6**(1), 21-27.

25 G. Zhu, G., M.F. Mehler, J. Zhao, S. Yu Yung and J.A. Kessler. "Sonic hedgehog and BMP2 exert opposing actions on proliferation and differentiation of embryonic neural progenitor cells," *Develop Bio,* 1999, **215**(1), 118-129.

26 N.M. Amankulor, D. Hambardzumyan, S.M. Pyonteck, et al. "Sonic hedgehog pathway activation is induced by acute brain injury and regulated by injury-related inflammation," *J Neurosci,* 2009, **29**: (33), 10299-10308.

27 N.I. Bamber, H. Li, X. Lu, et al. "Neurotrophins BDNF and NT3 promote axonal re-entry into the distal host spinal cord through Schwann cell-seeded mini-channels," *Eur J Neurosci,* 2001, **13**(2), 257-268.

28 B. Barres, M. Raff, F. Gaese, et al. "A crucial role for neurotrophin-3 in oligodendrocyte development," *Nature*, 1994, **367**, 371-375.

29 U. Engel and G. Wolswijk "Oligodendrocyte-type-2A astrocyte (O-2A) progenitor cells derived from adult rat spinal cord: In vitro characteristics and response to PDGF, bFGF and NT3," *Glia*, 1996, **16**(1), 16-26.

30 S. Kumar, M.A. Kahn, L. Dinh and J. de Vellis. "NT3-mediated TrkC receptor activation promotes proliferation and cell survival of rodent progenitor oligodendrocyte cells in vitro and in vivo," *J Neurosci Res,* 1998. **54**(6), 754-765.

31 D.M. McTigue, P.J. Horner, B.T. Stokes and F.H. Gage. "Neurotrophin-3 and brain-derived neurotrophic factor induce oligodendrocyte proliferation and myelination of regenerating axons in the contused adult rat spinal cord," *J Neurosci,* 1998, **18**(14), 5354-5365.

32 C.L. Wu, S.D. Chen, C.S. Hwang and D.I. Yang. "Sonic hedgehog mediates BDNF-induced neuroprotection against mitochondrial inhibitor 3-nitropropionic acid," *Biochem Biophys Res Commun,* 2009, **385**(1), 112-117.

33 J. Wu, S. Zhang and X. Sun. "Neuroprotective effect of upregulated sonic hedgehog in retinal ganglion cells following chronic ocular hypertension," *Invest Ophthalmol Visual Sci*, 2010, **51**(6), 2986-2992.

34 P. Merchan, A. Bribian, C. Sanchez-Camacho, et al. "Sonic hedgehog promotes the migration and proliferation of optic nerve oligodendrocyte precursors," *Mol Cell Neurosci,* 2007, **36**(3), 355-368.

35 C.H.H. Hor and B.L. Tang. "Sonic hedgehog as a chemoattractant for adult NPCs," *Cell Adhesion & Migration,* 2010, **4**(1), 1-3.

36 A.M. Thomas and L.D. Shea. "Polysaccharide-modified scaffolds for controlled lentivirus delivery in vitro and after spinal cord injury," *J Controlled Release,* 2013, **170**(3), 421-429.

37 S. Shin, H.M. Tuinstra, D.M. Salvay and L.D. Shea. "Phosphatidylserine immobilization of lentivirus for localized gene transfer," *Biomaterials,* 2010, **31**: (15), 4353-4359.

38 R. Cassiani-Ingoni, T. Coksaygan, H. Xue, et al. "Cytoplasmic translocation of Olig2 in adult glial progenitors marks the generation of reactive astrocytes following autoimmune inflammation," *Exp Neurol,* 2006, **201**(2), 349-358.

39 T. Magnus, T. Coksaygan, T. Korn, et al. "Evidence that nucleocytoplasmic Olig2 translocation mediates brain-injury-induced differentiation of glial precursors to astrocytes," *J Neurosci Res,* 2007, **85**(10), 2126-2137.

40 A. Foret, R. Quertainmont, O. Botman, et al. "Stem cells in the adult rat spinal cord: plasticity after injury and treadmill training exercise," *J Neurochem,* 2010, **112**(3), 762-772.

41 H.J. Lee, J. Wu, J. Chung and J.R. Wrathall. "SOX2 expression is upregulated in adult spinal cord after contusion injury in both oligodendrocyte lineage and ependymal cells," *J Neurosci Res*, 2013, **91**(2), 196-210.

42 C.Y. Brazel, T.L. Limke, J.K. Osborne, et al. "Sox2 expression defines a heterogeneous population of neurosphere-forming cells in the adult murine brain," *Aging Cell,* 2005, **4**(4), 197-207.

43 C.A. Marshall, B.G. Novitch and J.E. Goldman. "Olig2 directs astrocyte and oligodendrocyte formation in postnatal subventricular zone cells," *J Neurosci,* 2005, **25**(32), 7289-7298.

44 X. Tang, J.E. Davies and S.J.A. Davies. "Changes in distribution, cell associations, and protein expression levels of NG2, neurocan, phosphacan, brevican, versican V2, and tenascin-C during acute to chronic maturation of spinal cord scar tissue," *J Neurosci Res,* 2003, **71**: (3), 427-444.

45 D.M. McTigue, R. Tripathi and P. Wei. "NG2 colocalizes with axons and is expressed by a mixed cell population in spinal cord lesions," *J Neuropathol Exp Neurol,* 2006, **65**: (4), 406-420.

46 J. Yamauchi, J.R. Chan and E.M. Shooter. "Neurotrophins regulate Schwann cell migration by activating divergent signaling pathways dependent on Rho GTPases," *Proc Natl Acad Sci USA,* 2004, **101**(23), 8774-8779.

47 S.M. Hughes, F. Moussavi-Harami, S.L. Sauter and B.L. Davidson. "Viral-mediated gene transfer to mouse primary neural progenitor cells," *Mol Ther,* 2002, **5**(1), 16-24.

48 A.A. Abdellatif, J.L. Pelt, R.L. Benton, et al. "Gene delivery to the spinal cord: Comparison between lentiviral, adenoviral, and retroviral vector delivery systems," *J Neurosci Res,* 2006, **84**(3), 553-567.

49 D. Stamataki, F. Ulloa, S.V. Tsoni, A. Mynett and J. Briscoe. "A gradient of Gli activity mediates graded Sonic Hedgehog signaling in the neural tube," *Genes & Development*, 2005, **19**:626-641.

50 L. Taylor, L. Jones, M.H. Tuszynski and A. Blesch. Neurotrophin-3 gradients established by lentiviral gene delivery promote short-distance axonal bridging beyond cellular grafts in the injured spinal cord," *J Neurosci*, 2006, **26**(38):9713-9721.

51 J.Y. Park, S.K. Kim, D.H. Woo, E.J. Lee, J.H. Kim and S.H. Lee. "Differentiation of neural progenitor cells in a microfluidic chip-generated cytokine gradient," *Stem Cells*, 2009, **27**(11):2645-2654.

52 J.F. Bonner, A. Blesch, B. Neuhuber and I. Fischer. "Promoting directional axon growth from neural progenitors grafted into the injured spinal cord," *J Neurosci Res*, 2010, **88**:1182-1192.

53 M. Ballerman and K. Fouad. "Spontaneous locomotor recovery in spinal cord injured rats is accompanied by anatomical plasticity of reticulospinal fibers," *Eur J Neurosci*, 2006, **23**(8), 1988-1996.

54 F.M. Bareyre, M. Kerschensteiner, O. Raineteau, T.C. Mettenleiter, O. Weinmann and M.E. Schwab. "The injured spinal cord spontaneously forms a new intraspinal circuit in rats," *Nature Neurosci,* 2004, **7**(3), 269-277.

55 J. Beauparlant, R. van den Brand, Q. Barraud, et al. "Undirected compensatory plasticity contributes to neuronal dysfunctional after severe spinal cord injury," *Brain,* 2013, **136**: (11), 3347-3361.

56 A. Blesch and M.H. Tuszynski. "Spinal cord injury: Plasticity, regeneration and the challenge of translational drug development," *Trends Neurosci,* 2009, **32**(1), 41-47.

57 S. Rossignol "Plasticity of connections underlying locomotor recovery after central and/or peripheral lesions in the adult mammals," *Phil Trans Royal Soc B: Biol Sci*, 2006, **361**(1473), 1647-1671.

58 L. Taylor, L. Jones, M.H. Tuszynski and A. Blesch. "Neurotrophin-3 gradients established by lentiviral gene delivery promote short-distance axonal bridging beyond cellular grafts in the injured spinal cord," *J Neurosci,* 2006, **26**: (38), 9713-9721.

59 M. Neri, C. Maderna, D. Ferrari, et al. "Robust generation of oligodendrocyte progenitors from human neural stem cells and engraftment in experimental demyelination models in mice," *PloS One,* 2010, **5**: (4), e10145.

60 E. Binder, M. Rukavina, H. Hassani, et al. "Peripheral nervous system progenitors can be reprogrammed to produce myelinating oligodendrocytes and repair brain lesions," *J Neurosci,* 2011, **31**: (17), 6379-6391.

Figure Captions

Figure 1. (a) PLG bridge. (b) Schematic of bridge implantation into lateral hemisection injury. (c) Distribution of transgene expression along the spinal cord 4 weeks after injury (mean +/- SD). Note the bridge is implanted at T9/10. (d) Sustained expression of FLuc *in vivo* over 8 weeks with simultaneous delivery of GFP and FLuc lentiviral vectors from the bridge. Background signal remained less than $1x10^3$ photons/s during all measurements (e,f) Immunohistochemistry of spinal cord tissues extracted 8 weeks after injury with co-delivery of GFP and FLuc vectors (e) or bridge alone with no lentiviral delivery (f). Panels in (e) and (f) show staining for FLuc (upper left, red), GFP (upper right, green) and Hoescht (lower left, blue). are shown in the (green - GFP, upper right; red - FLuc, upper left; blue - Hoescht, lower right). Bottom right panels show overlaid images, where cell co-expressing GFP and FLuc appear yellow. Dashed lines denote the interface between bridge (left) implants and spinal cord tissue (right).

Fig. 2. $Sox2^+$(red)/$Hoescht^+$(blue) nuclei 8 wks after injury. (a) Immunofluorescence of $Sox2^+$ cells from bridge implants delivering lentivirus encoding SHH. Dashed line indicates border between bridge implant and host tissue. $Sox2^+$ immunofluorescence at higher magnification from bridges delivering (b) FLuc, (c) SHH, (d) NT3, or (e) NT3 and SHH. Arrows indicate $Sox2^+$ nuclei. (f) Quantification of $Sox2^+$ nuclei in FLuc, NT3, SHH and NT3+SHH conditions (mean +/- SD). (g) Quantification of sub-populations of $Sox2^+$/$Hoescht^+$ nuclei (co-expression of GFAP or Olig2) as a percentage of total $Sox2^+$/$Hoescht^+$ cells (mean +/- SD). (h) Quantification of sub-population densities of $Sox2^+$/$Hoescht^+$ nuclei (co-expression of GFAP or Olig2) (mean +/- SD).

Fig. 3. $Olig2^+$(red)/$Hoescht^+$(blue) nuclei 8 wks after injury. (a) Immunofluorescence of $Olig2^+$ cells from bridge implants delivering lentivirus encoding SHH. Dashed line indicates border between bridge implant and host tissue. Olig2+ Immunofluorescence at higher magnification from bridges delivering (b) FLuc, (c) SHH, (d) NT3, or (d) NT3 and SHH. Arrows indicate $Olig2^+$ nuclei. Brightness and contrast were adjusted for clarity. (e) Quantification of $Olig2^+$ nuclei in FLuc, NT3, SHH and NT3+SHH conditions (mean +/- SD). (f) Quantification of sub-populations of $Olig2^+$/$Hoescht^+$ nuclei (co-expression of GFAP or Sox2) as a percentage of total $Olig2^+$/ $Hoescht^+$ cells (mean +/- SD). (h) Quantification of sub-population densities of $Olig2^+$/$Hoescht^+$ nuclei (co-expression of GFAP or Sox2) (mean +/- SD).

Fig. 4. $GFAP^+$ cells (red) 8 wks after injury. (a) Immunofluorescence of $GFAP^+$ cells from bridge implants delivering lentivirus encoding SHH. Dashed line indicates border between bridge implant and host tissue. $GFAP^+$ immunofluorescence at higher magnification from bridges delivering (a) FLuc, (b) SHH, (c) NT3, or (d) NT3 and SHH. Interface between bridge and contralateral tissue is visible in each image. Arrows indicate $GFAP^+$ cells. Brightness and contrast were adjusted for clarity. (e) Quantification of $GFAP^+$ cells in FLuc, NT3, SHH and NT3+SHH conditions (mean +/- SD).

Fig. 5. Myelinated axons 8 wks after injury. (a) Immunofluorescence of myelinated (NFM^+/MBP^+: red/green, respectively) and total (NFM^+: red) axons from bridge implants delivering lentivirus encoding SHH. Dashed line indicates border between bridge implant and host tissue. NFM+/MBP^+ Immunofluorescence at higher magnification from bridges delivering (b) FLuc, (c) SHH, (d) NT3, or (e) NT3+SHH. White arrows show unmyelinated neurofilaments and yellow arrows show myelinated neurofilaments. Brightness and contrast were adjusted for clarity. (f) Quantification of total axon numbers in FLuc, NT3, SHH and NT3+SHH conditions (mean +/- SD). (g) Percentage of axons that were myelinated (mean +/- SD).

Fig. 6. Source of myelination. (a) Widefield view of immunofluorescence of Schwann cell- ($NFM^+/MBP^+/P0^+$: blue/red/green, respectively) and oligodendrocyte- ($NFM^+/MBP^+/P0^-$) derived myelin fibers from bridge implants delivering lentivirus encoding SHH. Dashed line indicates border between bridge implant and host tissue. Immunofluorescence at higher magnification from bridges delivering (b) FLuc, (c) SHH, (d) NT3, or (e) NT3+SHH. White arrows show fibers wrapped by Schwann cell-derived myelin and yellow arrows show fibers myelinated by oligodendrocytes. Brightness and contrast were adjusted for clarity. (f) Quantification of total axon numbers in FLuc, NT3, SHH and NT3 and SHH conditions (mean +/- SD). (g) Percentage of axons that were myelinated by oligodendrocytes (mean +/- SD).

Supp. Fig. 1: Quantification of ($Hoescht^+$, blue) and proliferative ($Ki67^+$, green) nuclei (mean +/- SD).

Supp. Fig. 2: Quantification of proliferative (Ki67+) (a) $Sox2^+$, (b) Olig2+ and (c) GFAP+ cells (mean +/- SD) in the bridge area 8 wks after injury when lentiviral particles encoding for either FLuc, SHH, NT3, or NT3 plus SHH were delivered from bridge implants. $Ki67^+$ cells were considered proliferative. White arrowheads indicate $Sox2^+$ cells, whereas yellow arrowheads indicate proliferative $Sox2^+$ cells (double positive for Ki67). Only cells where $Hoescht^+$ pixels overlapped $Sox2^+$, $Olig2^+$ or $GFAP^+$ pixels were counted.

Supp. Fig. 3: Maximum axial projection of confocal slices of the middle of the scaffold (~18 um section thickness). (a) Overlay of GFAP (red), Olig2 (green), Sox2 (magenta), and Hoescht (blue). Grayscale images of (b) GFAP, (c) Olig2, (d) Sox2 and (e) Hoescht (nuclei). White arrows indicate $Sox2^+/GFAP^+/Olig2^-$ cells, white asterisks indicate $Sox2^+/GFAP^-/Olig2^-$ cells, red arrows indicate $Olig2^+/GFAP^+/Sox2^-$ cells, red asterisks indicate $Olig2^+/GFAP^-/Sox2^-$ cells, blue arrows indicate $Sox2^+/GFAP^+/Olig2^+$ cells and blue asterisks indicate $Sox2^+/Olig2^+/GFAP^-$ cells.

Supp. Fig. 4: Markers for oligodendrogenesis 8 wks after injury in the presence of (a,e,i) Fluc, (b,f,j) SHH, (c,g,k) NT3, or (d,h,l) NT3 plus SHH. Tissue sections were stained for (a-d) $NG2^+$ (glial-restricted progenitors, meningeal fibroblasts, non-myelinating Schwann cells, and macrophages: red), (e-h) $O4^+$ (immature oligodendrocytes: green), and (i-l) $GalC^+$ (immature and mature oligodendrocytes: red) in the bridge. Proliferative cells were also $Ki67^+$, as indicated on the image. All images represent areas within the bridge implants. Yellow arrowheads indicate positive staining for the indicated markers, whereas white arrowheads indicate co-localization of the marker with Ki67.

Supp. Fig. 5: Representative images showing overlap of immunofluorescence markers with nuclei. (a-c) $Sox2^+$ cells were identified by co-localization of $Sox2^+$ (red) and $Hoescht^+$ (blue) nuclei in bridge implants. Arrows indicate examples of $Sox2^+$ cells. (d-f) $Olig2^+$ cells were identified by co-localization of $Olig2^+$ (red) and $Hoescht^+$ (blue) nuclei in bridge implants. Arrows indicate examples of $Olig2^+$ cells. (g-i) $GFAP^+$ cells were identified by overlap of $GFAP^+$ (red) cytoplasm and $Hosecht^+$ (blue) nuclei in bridge implants. Arrows indicate examples of $GFAP^+$ cells. Brightness and contrast were adjusted for clarity.

Supp. Fig. 6. Representative mmunofluorescence images demonstrating overlap of neurofilament and myelin markers. (a-c) NFM^+ (red) processes were identified as axons. Axonal processes co-labeled with MBP (green) were considered to be myelinated (white arrows). (d-g) NFM^+ (blue) processes were identified as axons. Axonal processes co-labeled with MBP (red), but not P0 (green) were considered to be myelinated by oligodendrocytes (yellow arrows), while NFM^+ processes positive for both MBP and P0 were considered to be myelinated by Schwann cells (white arrows). Brightness and contrast were adjusted for clarity.

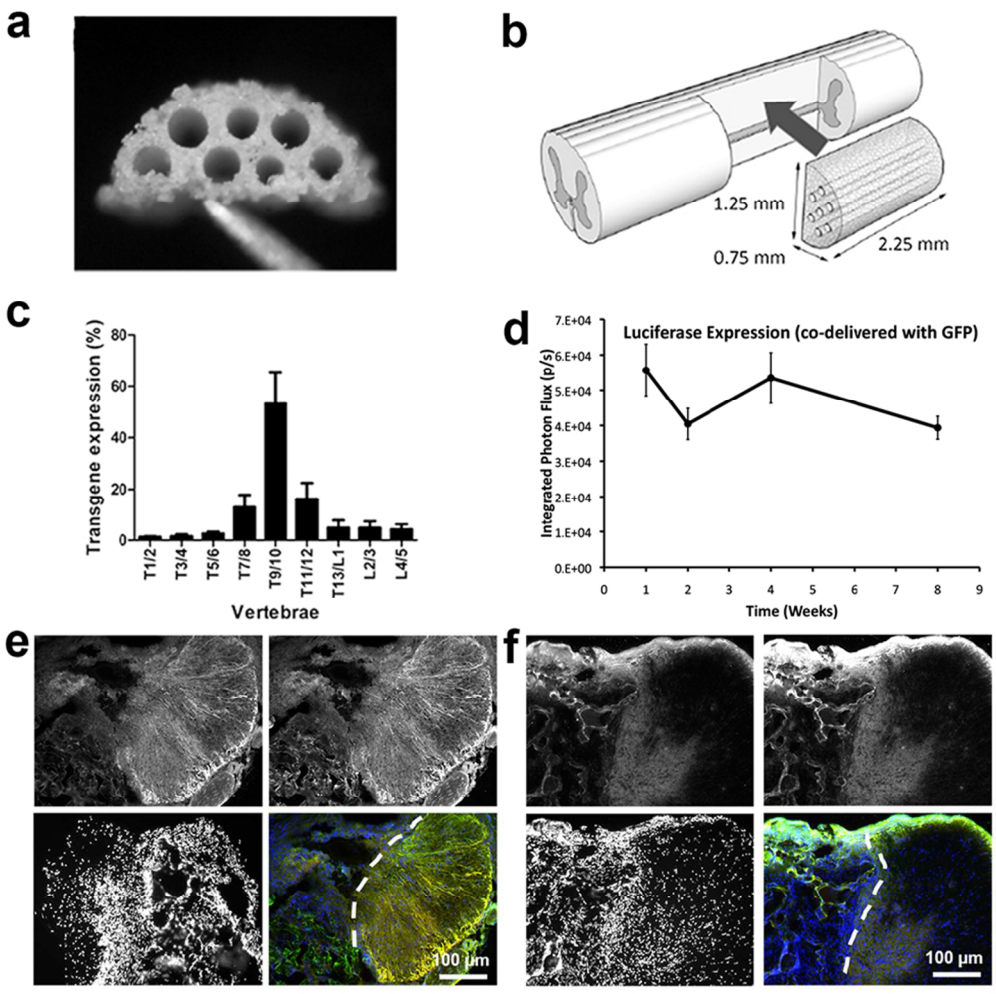

82x82mm (300 x 300 DPI)

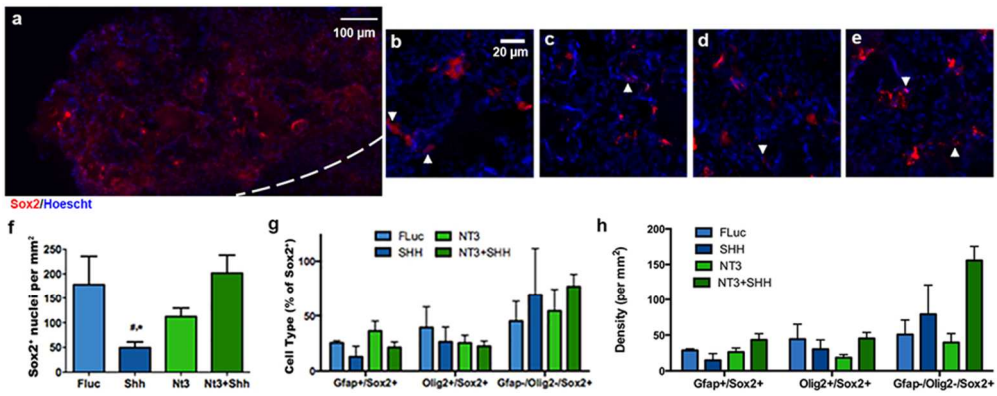

82x32mm (300 x 300 DPI)

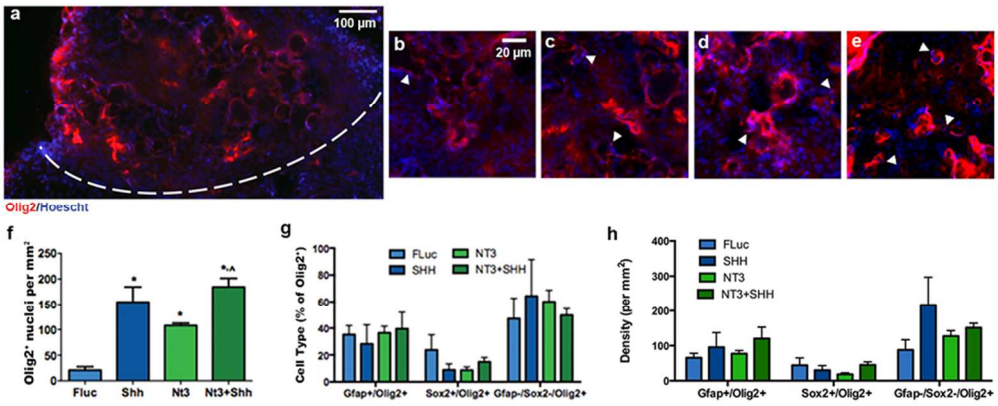

82x33mm (300 x 300 DPI)

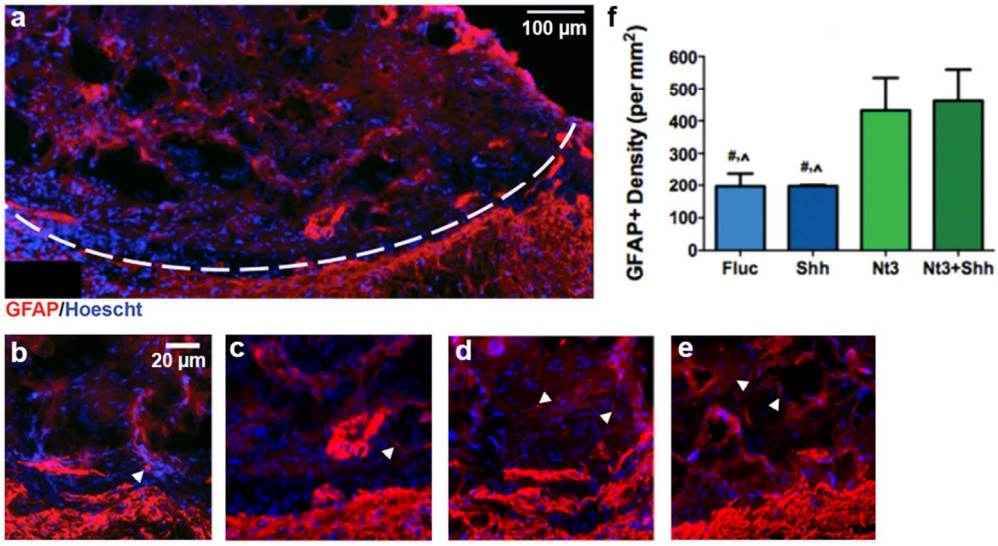

82x46mm (300 x 300 DPI)

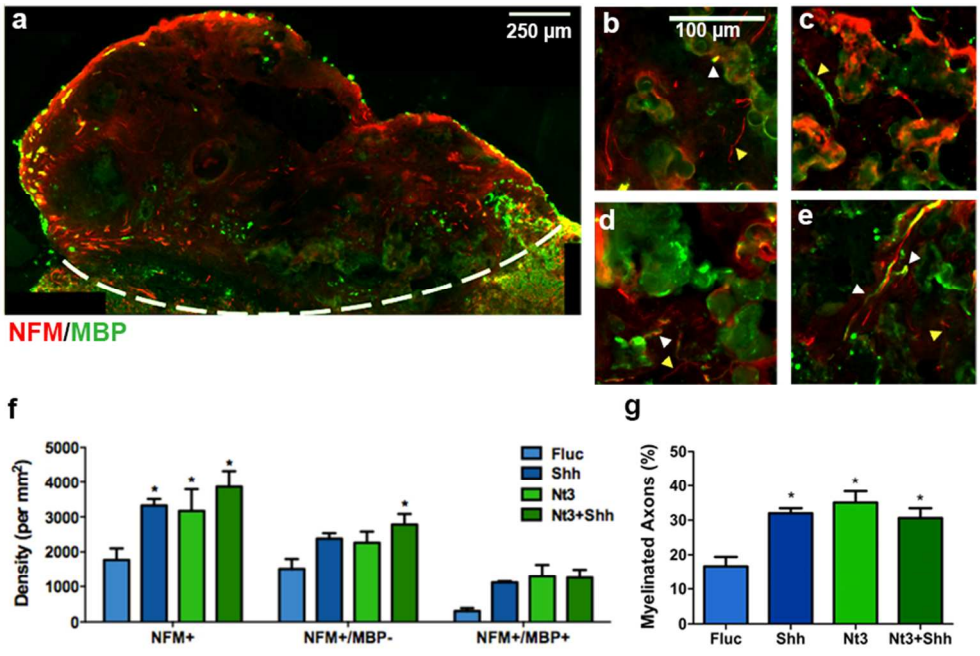

82x55mm (300 x 300 DPI)

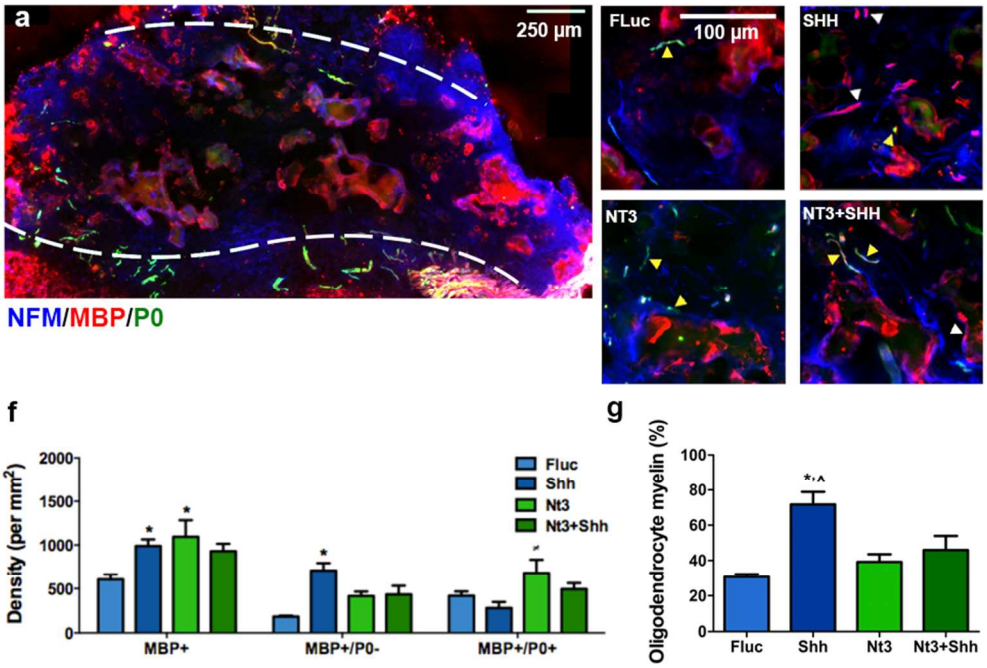

82x55mm (300 x 300 DPI)